Syracuse University
SURFACE

Electrical Engineering and Computer Science | L.C. Smith College of Engineering and Computer Science

2004

Solution of time domain PMCHW formulation for transient electromagnetic scattering from arbitrarily shaped 3-D dielectric objects

Baek Ho Jung
Hoseo University

T. K. Sarkar
Syracuse University

Y.-S. Chung
Myongji University

Follow this and additional works at: http://surface.syr.edu/eecs

Part of the Electrical and Computer Engineering Commons

Recommended Citation
Jung, Baek Ho; Sarkar, T. K.; and Chung, Y.-S., "Solution of time domain PMCHW formulation for transient electromagnetic scattering from arbitrarily shaped 3-D dielectric objects" (2004). *Electrical Engineering and Computer Science*. Paper 149.
http://surface.syr.edu/eecs/149

This Article is brought to you for free and open access by the L.C. Smith College of Engineering and Computer Science at SURFACE. It has been accepted for inclusion in Electrical Engineering and Computer Science by an authorized administrator of SURFACE. For more information, please contact surface@syr.edu.

Progress In Electromagnetics Research, PIER 45, 291–312, 2004

SOLUTION OF TIME DOMAIN PMCHW FORMULATION FOR TRANSIENT ELECTROMAGNETIC SCATTERING FROM ARBITRARILY SHAPED 3-D DIELECTRIC OBJECTS

B. H. Jung

Department of Information and Communication Engineering
Hoseo University
Asan, Chungnam 336-795, Korea

T. K. Sarkar

Department of Electrical Engineering and Computer Science
Syracuse University
Syracuse, NY 13244-1240, USA

Y.-S. Chung

Department of Communication Engineering
Myongji University
Yongin, Kyunggi 449-728, Korea

Abstract—In this paper, we analyze the transient electromagnetic response from three-dimensional (3-D) dielectric bodies using a time domain PMCHW (Poggio, Miller, Chang, Harrington, Wu) integral equation. The solution method in this paper is based on the Galerkin's method that involves separate spatial and temporal testing procedures. Triangular patch basis functions are used for spatial expansion and testing functions for arbitrarily shaped 3-D dielectric structures. The time domain unknown coefficients of the equivalent electric and magnetic currents are approximated by a set of orthonormal basis functions that are derived from the Laguerre functions. These basis functions are also used as the temporal testing. Use of the Laguerre polynomials as expansion functions characterizing the time variable enables one to handle the time derivative terms in the integral equation and decouples the space-time continuum in an analytic fashion. We also propose an alternative formulation using a differential form of time domain PMCHW equation with a different expansion for the equivalent currents. Numerical results computed by the two proposed methods are presented and compared.

1 Introduction

2 Formulation

2.1 Spatial Expansion and Testing

2.2 Temporal Expansion and Testing

2.3 Equivalent Currents and Far Field

3 Alternative Formulation

4 Numerical Examples

5 Conclusion

References

1. INTRODUCTION

For the solution of the transient scattering from conducting and dielectric objects using time domain integral equations, the marching-on in time (MOT) technique is extensively employed [1]. A serious drawback of this algorithm is the occurrence of late-time instabilities in the form of high frequency oscillation. Several MOT formulations have been presented for the solution of the electromagnetic scattering from arbitrarily shaped 3-D dielectric structures using triangular patch modeling technique [2–4]. An explicit solution of the time domain PMCHW formulation has been presented by differentiating the coupled integral equations and using second order finite difference [2]. But the results become unstable for late times. The late-time oscillations could be eliminated by approximating the average value of the current. In addition, a backward finite difference approximation for the magnetic vector potential term in the time domain electric field integral equation has been used for the implicit technique to minimize these late-time oscillations [3, 4]. Even though employing the implicit technique, the solution obtained by using MOT has still a late-time oscillation that is dependent on the choice of the time step.

In this paper, we present a new technique to obtain stable responses of the time domain PMCHW formulation for arbitrarily shaped 3-D dielectric objects using Laguerre polynomials as temporal basis functions. The Laguerre series is defined only over the interval from zero to infinity, and hence, are considered to be more suited for the transient problem, as they naturally enforce causality. Using the Laguerre polynomials, we construct a set of orthonormal basis functions [5]. Transient quantities that are functions of time can be spanned in terms of these orthogonal basis functions. The temporal basis functions used in this work are completely convergent to zero

as time increases to infinity. Therefore, transient response spanned by these basis functions is also convergent to zero as time progresses. Using Galerkin's method, we introduce a temporal testing procedure, which is similar to the spatial testing procedure of the method of moments (MoM). By applying the temporal testing to the time domain integral equations, we can eliminate the numerical instabilities. Instead of the MOT procedure, we employ a marching-on in-degree procedure by increasing the degree of the temporal testing functions. Therefore, we can obtain the unknown coefficients of the expansion by solving a matrix equation recursively with a finite number of basis functions.

In the next section, we describe the time domain PMCHW formulation and set up a matrix equation by applying MoM with spatial and temporal testing procedures. Section 3 describes an alternative technique using a differential form of the coupled integral equations with a different expansion for the equivalent currents. Section 4 presents and compares numerical results followed by Section 5, the conclusion.

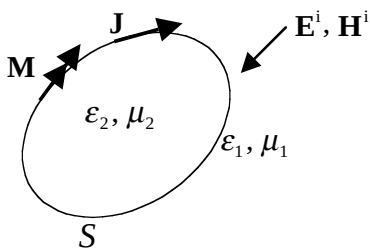

Figure 1. Homogeneous dielectric body illuminated by an electromagnetic pulse.

2. FORMULATION

In this section, we discuss the time domain PMCHW formulation and derive a matrix equation to obtain induced equivalent currents on a dielectric scatterer, which is illuminated by an electromagnetic pulse. We consider a homogeneous dielectric body with a permittivity ε_2 and a permeability μ_2 placed in an infinite homogeneous medium with a permittivity ε_1 and a permeability μ_1, as shown in Fig. 1. By invoking the equivalence principle, the integral equation is formulated in terms of the equivalent electric and magnetic current $\boldsymbol{J}$ and $\boldsymbol{M}$ on the surface S of the dielectric body. By enforcing the continuity of the tangential electric and magnetic field at S, the following PMCHW

integral equations are obtained:

$$\sum_{v=1}^{2}\left[\frac{\partial}{\partial t}\boldsymbol{A}_v(\boldsymbol{r},t)+\nabla\Phi_v(\boldsymbol{r},t)+\frac{1}{\varepsilon_v}\nabla\times\boldsymbol{F}_v(\boldsymbol{r},t)\right]_{\tan}=[\boldsymbol{E}^{\mathrm{i}}(\boldsymbol{r},t)]_{\tan},\ \boldsymbol{r}\in S \tag{1}$$

$$\sum_{v=1}^{2}\left[\frac{\partial}{\partial t}\boldsymbol{F}_v(\boldsymbol{r},t)+\nabla\Psi_v(\boldsymbol{r},t)-\frac{1}{\mu_v}\nabla\times\boldsymbol{A}_v(\boldsymbol{r},t)\right]_{\tan}=[\boldsymbol{H}^{\mathrm{i}}(\boldsymbol{r},t)]_{\tan},\ \boldsymbol{r}\in S \tag{2}$$

where v is 1 or 2, $\boldsymbol{E}^{\mathrm{i}}$ and $\boldsymbol{H}^{\mathrm{i}}$ are the incident electric and magnetic fields, respectively. The subscript 'tan' denotes the tangential component. In (1) and (2), $\boldsymbol{A}_v$ and $\boldsymbol{F}_v$ are the magnetic and electric vector potentials, respectively, and Φ_v and Ψ_v are the electric and magnetic scalar potentials given by

$$\boldsymbol{A}_v(\boldsymbol{r},t) = \frac{\mu_v}{4\pi}\int_S \frac{\boldsymbol{J}(\boldsymbol{r}',\tau_v)}{R}dS' \tag{3}$$

$$\boldsymbol{F}_v(\boldsymbol{r},t) = \frac{\varepsilon_v}{4\pi}\int_S \frac{\boldsymbol{M}(\boldsymbol{r}',\tau_v)}{R}dS' \tag{4}$$

$$\Phi_v(\boldsymbol{r},t) = \frac{1}{4\pi\varepsilon_v}\int_S \frac{q_e(\boldsymbol{r}',\tau_v)}{R}dS' \tag{5}$$

$$\Psi_v(\boldsymbol{r},t) = \frac{1}{4\pi\mu_v}\int_S \frac{q_m(\boldsymbol{r}',\tau_v)}{R}dS' \tag{6}$$

where $R=|\boldsymbol{r}-\boldsymbol{r}'|$ represents the distance between the arbitrarily located observation point $\boldsymbol{r}$ and the source point $\boldsymbol{r}'$, $\tau_v = t - R/c_v$ is the retarded time, and $c_v = 1/\sqrt{\varepsilon_v\mu_v}$ is the velocity of propagation of the electromagnetic wave in the space with medium parameters (ε_v,μ_v). The electric and magnetic surface charge density q_e and q_m are related to the electric and magnetic current density by the equation of continuity, respectively,

$$\nabla\cdot\boldsymbol{J}(\boldsymbol{r},t) = -\frac{\partial}{\partial t}q_e(\boldsymbol{r},t) \tag{7}$$

$$\nabla\cdot\boldsymbol{M}(\boldsymbol{r},t) = -\frac{\partial}{\partial t}q_m(\boldsymbol{r},t) \tag{8}$$

The integral equations described by (1) and (2) consist of the combined field integral equation since we enforced the continuity condition on the electric and magnetic fields.

2.1. Spatial Expansion and Testing

The surface of the dielectric structure to be analyzed is approximated by planar triangular patches. As in [6], we define the spatial basis function associated with the n-th common edge as

$$\boldsymbol{f}_n(\boldsymbol{r}) = \boldsymbol{f}_n^+(\boldsymbol{r}) + \boldsymbol{f}_n^-(\boldsymbol{r}) \tag{9a}$$

$$\boldsymbol{f}_n^\pm(\boldsymbol{r}) = \begin{cases} \dfrac{l_n}{2A_n^\pm}\boldsymbol{\rho}_n^\pm, & \boldsymbol{r} \in T_n^\pm \\ 0, & \boldsymbol{r} \notin T_n^\pm \end{cases} \tag{9b}$$

where l_n and $A_n^\pm$ are the length of the edge and the area of triangle $T_n^\pm$. $\boldsymbol{\rho}_n^\pm$ is the position vector defined with respect to the free vertex of $T_n^\pm$. In general, the electric current $\boldsymbol{J}$ and the magnetic current $\boldsymbol{M}$ on the dielectric structure may be approximated in terms of this spatial basis function as

$$\boldsymbol{J}(\boldsymbol{r},t) = \sum_{n=1}^{N} J_n(t)\boldsymbol{f}_n(\boldsymbol{r}) \tag{10}$$

$$\boldsymbol{M}(\boldsymbol{r},t) = \sum_{n=1}^{N} M_n(t)\boldsymbol{f}_n(\boldsymbol{r}) \tag{11}$$

where J_n and M_n are constants yet to be determined and N is the number of edges on the surface for the triangulated model approximating the surface of the dielectric body. When (5) and (6) are used in (1) and (2), we encounter time-integral terms which are due to (7) and (8). For convenience and to avoid the computation of the time derivatives numerically, we evaluate the time derivative of the vector potential in (1) and (2) analytically. We introduce new source vectors $\boldsymbol{e}$ and $\boldsymbol{h}$ defined by

$$\boldsymbol{J}(\boldsymbol{r},t) = \frac{\partial}{\partial t}\boldsymbol{e}(\boldsymbol{r},t) \tag{12}$$

$$\boldsymbol{M}(\boldsymbol{r},t) = \frac{\partial}{\partial t}\boldsymbol{h}(\boldsymbol{r},t) \tag{13}$$

where the relation between these source vectors and the charge densities are given through

$$q_e(\boldsymbol{r},t) = -\nabla\cdot\boldsymbol{e}(\boldsymbol{r},t) \tag{14}$$

$$q_m(\boldsymbol{r},t) = -\nabla\cdot\boldsymbol{h}(\boldsymbol{r},t). \tag{15}$$

By using (9), we may expand the two source vectors as

$$\boldsymbol{e}(\boldsymbol{r},t) = \sum_{n=1}^{N} e_n(t)\boldsymbol{f}_n(\boldsymbol{r}) \tag{16}$$

$$\boldsymbol{h}(\boldsymbol{r},t) = \sum_{n=1}^{N} h_n(t)\boldsymbol{f}_n(\boldsymbol{r}) \tag{17}$$

where e_n and h_n are the time-domain unknown coefficients to be determined.

The next step in the numerical implementation scheme is to develop a testing procedure to transform the operator equations (1) and (2) into a matrix equation using the MoM. First, we consider the testing of (1). By substituting (3)–(5) and (12)–(14) into (1) with (16) and (17), and choosing the expansion function $\boldsymbol{f}_m$ also as testing functions with the standard definition of the inner product, we have

$$\sum_{v=1}^{2}\sum_{n=1}^{N}\sum_{p,q}\left[\mu_v a_{mn}^{pq}\frac{d^2}{dt^2}e_n(\tau_{mn,v}^{pq}) + \frac{b_{mn}^{pq}}{\varepsilon_v}e_n(\tau_{mn,v}^{pq})\right.$$
$$\left. + \frac{I_1^{pq}}{c_v}\frac{d^2}{dt^2}h_n(\tau_{mn,v}^{pq}) + I_2^{pq}\frac{d}{dt}h_n(\tau_{mn,v}^{pq})\right] = V_m^E(t),\ m = 1,2,\ldots,N \tag{18}$$

where

$$a_{mn}^{pq} = \frac{1}{4\pi}\int_S \boldsymbol{f}_m^p(\boldsymbol{r})\cdot\int_S \frac{\boldsymbol{f}_n^q(\boldsymbol{r}')}{R}dS'dS \tag{19}$$

$$b_{mn}^{pq} = \frac{1}{4\pi}\int_S \nabla\cdot\boldsymbol{f}_m^p(\boldsymbol{r})\int_S \frac{\nabla'\cdot\boldsymbol{f}_n^q(\boldsymbol{r}')}{R}dS'dS \tag{20}$$

$$I_k^{pq} = \frac{1}{4\pi}\int_S \boldsymbol{f}_m^p(\boldsymbol{r})\cdot\int_S \boldsymbol{f}_n^q(\boldsymbol{r}')\times\frac{\hat{\boldsymbol{R}}}{R^k}dS'dS,\ k = 1,2 \tag{21}$$

$$V_m^E(t) = \int_S \boldsymbol{f}_m(\boldsymbol{r})\cdot\boldsymbol{E}^{\mathrm{i}}(\boldsymbol{r},t)dS. \tag{22}$$

In (21), $\hat{\boldsymbol{R}}$ is a unit vector along the direction $\boldsymbol{r}-\boldsymbol{r}'$. The integrals (19) and (20) may be evaluated by the method described in [6] and [7]. The integral in (21) may be evaluated using the Gaussian quadrature integral scheme for unprimed and primed coordinates numerically. In deriving (18), we assumed that the functions dependent on the following variable do not change appreciably within a given triangular patch so that

$$\tau_v = t - \frac{R}{c_v} \rightarrow \tau_{mn,v}^{pq} = t - \frac{R_{mn}^{pq}}{c_v},\quad R_{mn}^{pq} = |\boldsymbol{r}_m^{cp} - \boldsymbol{r}_n^{cq}|$$

where p and q are $+$ or $-$. $\boldsymbol{r}_n^{c\pm}$ is the position vector of the center in triangle $T_n^{\pm}$.

2.2. Temporal Expansion and Testing

Now, we consider the choice of the temporal basis functions and the temporal testing procedure. An orthonormal basis function set can be derived from the Laguerre functions through the representation [5]

$$\phi_j(t) = e^{-t/2} L_j(t) \tag{23}$$

where L_j is the Laguerre polynomial of degree j. They are causal, i.e., exist for $t \geq 0$. The coefficients for the temporal expansion functions $e_n(t)$ and $h_n(t)$ introduced in (16) and (17) are assumed to be causal electromagnetic response functions for $t \geq 0$. They can be expanded using (23) as

$$a_n(t) = \sum_{j=0}^{\infty} a_{n,j} \phi_j(st) \tag{24}$$

where $a_n(t)$ represents $e_n(t)$ or $h_n(t)$, $a_{n,j}$ is the coefficient to be determined, and s is a scaling factor. Using the orthogonality of (23) [8], the expressions for the first and the second derivatives can be written explicitly using the time domain coefficient and are given by

$$\frac{d}{dt} a_n(t) = s \sum_{j=0}^{\infty} \left[\frac{1}{2} a_{n,j} + \sum_{k=0}^{j-1} a_{n,k} \right] \phi_j(st) \tag{25}$$

$$\frac{d^2}{dt^2} a_n(t) = s^2 \sum_{j=0}^{\infty} \left[\frac{1}{4} a_{n,j} + \sum_{k=0}^{j-1} (j-k) a_{n,k} \right] \phi_j(st). \tag{26}$$

Substituting the expressions of expansion of the unknown and their derivatives (24)–(26) into (18), and performing a temporal testing, which means multiplying $\phi_i(st)$ and integrating from zero to infinity, we get

$$\begin{aligned} &\sum_{v=1}^{2} \sum_{n=1}^{N} \sum_{p,q} \sum_{j=0}^{\infty} \left[\left\{ \left(\frac{s^2}{4} \mu_v a_{mn}^{pq} + \frac{b_{mn}^{pq}}{\varepsilon_v} \right) e_{n,j} + s^2 \mu_v a_{mn}^{pq} \sum_{k=0}^{j-1} (j-k) e_{n,k} \right\} \right. \\ &\cdot I_{ij}\left(s \frac{R_{mn}^{pq}}{c_v} \right) \left\{ \left(\frac{s^2}{4} \frac{I_1^{pq}}{c_v} + \frac{s}{2} I_2^{pq} \right) h_{n,j} + \sum_{k=0}^{j-1} \left(s^2 \frac{I_1^{pq}}{c_v} (j-k) + s I_2^{pq} \right) h_{n,k} \right\} \\ &\left. \cdot\, I_{ij}\left(s \frac{R_{mn}^{pq}}{c_v} \right) \right] = V_{m,i}^{E} \end{aligned} \tag{27}$$

where $e_{n,j}$ and $h_{n,j}$ are unknown coefficients related to the $e_n(t)$ and $h_n(t)$, respectively, and

$$I_{ij}\left(s \frac{R_{mn}^{pq}}{c_v} \right) = \int_0^{\infty} \phi_i(st) \phi_j\left(st - s \frac{R_{mn}^{pq}}{c_v} \right) d(st) \tag{28}$$

$$V_{m,i}^E = \int_0^\infty \phi_i(st) V_m^E(t) d(st). \tag{29}$$

Using the formula (8.971) and (8.974) in [9], the integral (28) can be computed as

$$I_{ij}(y) = \begin{cases} \phi_{i-j}(y) - \phi_{i-j-1}(y), & j \le i \\ 0, & j > i \end{cases} \tag{30}$$

where $y = sR_{mn}^{pq}/c_v$.

We note that $I_{ij} = 0$ when $j > i$ from (30). Therefore we can write the upper limit for the summation over j as i instead of ∞ in (27). By moving the terms associated with $e_{n,j}$ and $h_{n,j}$, which are known for $j < i$, to the right-hand side, we obtain

$$\sum_{n=1}^{N} \left(\alpha_{mn}^E e_{n,i} + \beta_{mn}^E h_{n,i} \right) = V_{m,i}^E + P_{m,i}^E + Q_{m,i}^E \tag{31}$$

where

$$\alpha_{mn}^E = \sum_{v=1}^{2} \sum_{p,q} \left(\frac{s^2}{4} \mu_v a_{mn}^{pq} + \frac{b_{mn}^{pq}}{\varepsilon_v} \right) \exp\left(-s \frac{R_{mn}^{pq}}{2c_v} \right) \tag{32}$$

$$\beta_{mn}^E = \sum_{v=1}^{2} \sum_{p,q} \left(\frac{s^2}{4} \frac{I_1^{pq}}{c_v} + \frac{s}{2} I_2^{pq} \right) \exp\left(-s \frac{R_{mn}^{pq}}{2c_v} \right) \tag{33}$$

$$\begin{aligned} P_{m,i}^E = & -\sum_{v=1}^{2} \sum_{n=1}^{N} \sum_{p,q} \left[\left(\frac{s^2}{4} \mu_v a_{mn}^{pq} + \frac{b_{mn}^{pq}}{\varepsilon_v} \right) \sum_{j=0}^{i-1} e_{n,j} I_{ij} \left(s \frac{R_{mn}^{pq}}{c_v} \right) \right. \\ & \left. + s^2 \mu_v a_{mn}^{pq} \sum_{j=0}^{i} \sum_{k=0}^{j-1} (j-k) e_{n,k} I_{ij} \left(s \frac{R_{mn}^{pq}}{c_v} \right) \right] \end{aligned} \tag{34}$$

$$\begin{aligned} Q_{m,i}^E = & -\sum_{v=1}^{2} \sum_{n=1}^{N} \sum_{p,q} \left\{ \left(\frac{s^2}{4} \frac{I_1^{pq}}{c_v} + \frac{s}{2} I_2^{pq} \right) \sum_{j=0}^{i-1} h_{n,j} I_{ij} \left(s \frac{R_{mn}^{pq}}{c_v} \right) \right. \\ & + s^2 \frac{I_1^{pq}}{c_v} \sum_{j=0}^{i} \sum_{k=0}^{j-1} (j-k) h_{n,k} I_{ij} \left(s \frac{R_{mn}^{pq}}{c_v} \right) \\ & \left. + s I_2^{pq} \sum_{j=0}^{i} \sum_{k=0}^{j-1} h_{n,k} I_{ij} \left(s \frac{R_{mn}^{pq}}{c_v} \right) \right\} \end{aligned} \tag{35}$$

Using a similar procedure to derive (31) from (1) or applying a duality

theorem, we obtain the following from (2) as

$$\sum_{n=1}^{N}\left(\alpha_{mn}^{H}h_{n,i}+\beta_{mn}^{H}e_{n,i}\right)=V_{m,i}^{H}+P_{m,i}^{H}+Q_{m,i}^{H} \tag{36}$$

where

$$\alpha_{mn}^{H} = \sum_{v=1}^{2}\sum_{p,q}\left(\frac{s^2}{4}\varepsilon_v a_{mn}^{pq}+\frac{b_{mn}^{pq}}{\mu_v}\right)\exp\left(-s\frac{R_{mn}^{pq}}{2c_v}\right) \tag{37}$$

$$\beta_{mn}^{H} = -\sum_{v=1}^{2}\sum_{p,q}\left(\frac{s^2}{4}\frac{I_1^{pq}}{c_v}+\frac{s}{2}I_2^{pq}\right)\exp\left(-s\frac{R_{mn}^{pq}}{2c_v}\right) \tag{38}$$

$$\begin{aligned} P_{m,i}^{H} = & -\sum_{v=1}^{2}\sum_{n=1}^{N}\sum_{p,q}\left[\left(\frac{s^2}{4}\varepsilon_v a_{mn}^{pq}+\frac{b_{mn}^{pq}}{\mu_v}\right)\sum_{j=0}^{i-1}h_{n,j}I_{ij}\left(s\frac{R_{mn}^{pq}}{c_v}\right)\right. \\ & \left.+\, s^2\varepsilon_v a_{mn}^{pq}\sum_{j=0}^{i}\sum_{k=0}^{j-1}(j-k)h_{n,k}I_{ij}\left(s\frac{R_{mn}^{pq}}{c_v}\right)\right] \end{aligned} \tag{39}$$

$$\begin{aligned} Q_{m,i}^{H} = & \sum_{v=1}^{2}\sum_{n=1}^{N}\sum_{p,q}\left[\left(\frac{s^2}{4}\frac{I_1^{pq}}{c_v}+\frac{s}{2}I_2^{pq}\right)\sum_{j=0}^{i-1}e_{n,j}I_{ij}\left(s\frac{R_{mn}^{pq}}{c_v}\right)\right. \\ & +s^2\frac{I_1^{pq}}{c_v}\sum_{j=0}^{i}\sum_{k=0}^{j-1}(j-k)e_{n,k}I_{ij}\left(s\frac{R_{mn}^{pq}}{c_v}\right) \\ & \left.+\, sI_2^{pq}\sum_{j=0}^{i}\sum_{k=0}^{j-1}e_{n,k}I_{ij}\left(s\frac{R_{mn}^{pq}}{c_v}\right)\right] \end{aligned} \tag{40}$$

$$V_{m,i}^{H} = \int_0^{\infty}\phi_i(st)V_m^H(t)d(st) \tag{41}$$

$$V_m^H(t) = \int_S \boldsymbol{f}_m(\boldsymbol{r})\cdot\boldsymbol{H}^{\mathrm{i}}(\boldsymbol{r},t)dS \tag{42}$$

We can write (31) and (36) in a matrix equation as

$$\begin{bmatrix} \left[\alpha_{mn}^{E}\right] & \left[\beta_{mn}^{E}\right] \\ \left[\beta_{mn}^{H}\right] & \left[\alpha_{mn}^{H}\right] \end{bmatrix}\begin{bmatrix} [e_{n,i}] \\ [h_{n,i}] \end{bmatrix} = \begin{bmatrix} \left[\gamma_{m,i}^{E}\right] \\ \left[\gamma_{m,i}^{H}\right] \end{bmatrix}, \quad i=0,1,2,\ldots,\infty \tag{43}$$

where $\gamma_{m,i}^{E} = V_{m,i}^{E}+P_{m,i}^{E}+Q_{m,i}^{E}$ and $\gamma_{m,i}^{H} = V_{m,i}^{H}+P_{m,i}^{H}+Q_{m,i}^{H}$. We need the minimum degree or number of temporal basis functions,

M, in computing (43). This parameter is dependent on the time duration of the transient response and the bandwidth of the excitation signal. When we consider a signal with a frequency bandwidth B in the frequency domain and the time duration T_f in the time domain, the minimum number of temporal basis functions to approximate the transient signal becomes $M = 2BT_f + 1$ [5]. We note that the upper limit of the integral in (29) and (41) can be replaced by the time duration sT_f instead of infinity.

2.3. Equivalent Currents and Far Field

By solving the matrix equation (43) in a marching-on in degree manner with M temporal basis functions, the electric and magnetic transient current coefficients in (10) and (11) are expressed using the relation (12) and (13) with (25) as, respectively,

$$J_n(t) = \frac{\partial}{\partial t} e_n(t) = s \sum_{j=0}^{M-1} \left(\frac{1}{2} e_{n,j} + \sum_{k=0}^{j-1} e_{n,k} \right) \phi_j(st) \tag{44}$$

$$M_n(t) = \frac{\partial}{\partial t} h_n(t) = s \sum_{j=0}^{M-1} \left(\frac{1}{2} h_{n,j} + \sum_{k=0}^{j-1} h_{n,k} \right) \phi_j(st). \tag{45}$$

Once the coefficients of equivalent currents on the dielectric scatterer have been determined, we can compute the far scattered fields. These fields may be thought as the superposition of the fields due to the electric currents only and with the fields due to the magnetic currents only. We explain the analytic method to compute the far fields directly by using the coefficient $e_n(t)$ and $h_n(t)$ obtained from (43). The scattered field due to the electric currents alone at a point $\boldsymbol{r}$ is given by

$$\boldsymbol{E}^{\mathrm{s}}_{\boldsymbol{J}}(\boldsymbol{r}, t) \approx -\frac{\partial}{\partial t} \boldsymbol{A}_1(\boldsymbol{r}, t) \tag{46}$$

where the subscript $\boldsymbol{J}$ refers to the field due to the electric current. Substituting (3), (12), and (16) into (46) with (9a), we get

$$\boldsymbol{E}^{\mathrm{s}}_{\boldsymbol{J}}(\boldsymbol{r}, t) \approx -\frac{\mu_1}{4\pi} \sum_{n=1}^{N} \sum_{q} \int_S \frac{d^2}{dt^2} e_n \left(t - \frac{R}{c_1} \right) \frac{\boldsymbol{f}^q_n(\boldsymbol{r}')}{R} dS'. \tag{47}$$

We make the following approximations for the far field calculations:

$$R \approx r - \boldsymbol{r}' \cdot \hat{\boldsymbol{r}} \qquad \text{for the time retardation term } t - R/c_1$$
$$R \approx r \qquad \text{for the amplitude term } 1/R$$

where $\hat{\boldsymbol{r}} = \boldsymbol{r}/r$ is a unit vector in the direction of the radiation and c_1 is the velocity of light in medium 1. The integral in (47) is evaluated by approximating the integrand by the value at the center of the source triangle T_n^q. Substituting (9b) into (47) and approximating $\boldsymbol{r}' \approx \boldsymbol{r}_n^{cq}$ and $\boldsymbol{\rho}_n^q \approx \boldsymbol{\rho}_n^{cq}$, we obtain

$$\boldsymbol{E}_{\boldsymbol{J}}^{\mathrm{s}}(\boldsymbol{r},t) \approx -\frac{\mu_1}{8\pi r}\sum_{n=1}^{N} l_n \sum_q \boldsymbol{\rho}_n^{cq}\frac{d^2}{dt^2}e_n(\tau_n^q) \tag{48}$$

where $\tau_n^q \approx t - (r - \boldsymbol{r}_n^{cq}\cdot\hat{\boldsymbol{r}})/c_1$.

The scattered magnetic field is given by

$$\boldsymbol{H}_{\boldsymbol{M}}^{\mathrm{s}}(\boldsymbol{r},t) \approx -\frac{\partial}{\partial t}\boldsymbol{F}_1(\boldsymbol{r},t) \tag{49}$$

where the subscript $\boldsymbol{M}$ refers to the field due to the magnetic current. By following a similar analysis as that for the electric current or applying the duality theorem to (47), the far magnetic field is given by

$$\begin{aligned}\boldsymbol{H}_{\boldsymbol{M}}^{\mathrm{s}}(\boldsymbol{r},t) &\approx -\frac{\varepsilon_1}{4\pi}\sum_{n=1}^{N}\sum_q \int_S \frac{d^2}{dt^2}h_n\left(t-\frac{R}{c_1}\right)\frac{\boldsymbol{f}_n^q(\boldsymbol{r}')}{R}dS' \\ &= -\frac{\varepsilon_1}{8\pi r}\sum_{n=1}^{N} l_n \sum_q \boldsymbol{\rho}_n^{cq}\frac{d^2}{dt^2}h_n(\tau_n^q).\end{aligned} \tag{50}$$

From (50), the electric field is

$$\boldsymbol{E}_{\boldsymbol{M}}^{\mathrm{s}}(\boldsymbol{r},t) = \eta_1 \boldsymbol{H}_{\boldsymbol{M}}^{\mathrm{s}}(\boldsymbol{r},t)\times\hat{\boldsymbol{r}} \tag{51}$$

where η_1 is the wave impedance in the medium surrounding the scatterer. Finally the total field scattered from the dielectric body may be obtained by adding (48) and (51) with (50) as

$$\boldsymbol{E}^{\mathrm{s}}(\boldsymbol{r},t) \approx -\frac{1}{8\pi c_1 r}\left(\eta_1\sum_{n=1}^{N}\boldsymbol{A}_n + \sum_{n=1}^{N}\boldsymbol{F}_n\times\hat{\boldsymbol{r}}\right) \tag{52}$$

where

$$\boldsymbol{A}_n = l_n\sum_q \boldsymbol{\rho}_n^q\frac{d^2}{dt^2}e_n(\tau_n^q) \tag{53}$$

$$\boldsymbol{F}_n = l_n\sum_q \boldsymbol{\rho}_n^q\frac{d^2}{dt^2}h_n(\tau_n^q). \tag{54}$$

The second derivative of the time-domain coefficient is obtained from (26) with $M-1$ as the upper limit of summation over j instead of ∞.

3. ALTERNATIVE FORMULATION

In this section, we present an alternative method using the expansion for the equivalent currents directly instead of using the two source vectors. Taking a derivative with respect to time, we derive the following integral equations from (1) and (2)

$$\begin{aligned}&\sum_{v=1}^{2}\left[\frac{\partial^2}{\partial t^2}\boldsymbol{A}_v(\boldsymbol{r},t)+\nabla\frac{\partial}{\partial t}\Phi_v(\boldsymbol{r},t)+\frac{1}{\varepsilon_v}\nabla\times\frac{\partial}{\partial t}\boldsymbol{F}_v(\boldsymbol{r},t)\right]_{\tan}\\ =&\left[\frac{\partial}{\partial t}\boldsymbol{E}^{\mathrm{i}}(\boldsymbol{r},t)\right]_{\tan},\ \boldsymbol{r}\in S \qquad (55)\\ &\sum_{v=1}^{2}\left[\frac{\partial^2}{\partial t^2}\boldsymbol{F}_v(\boldsymbol{r},t)+\nabla\frac{\partial}{\partial t}\Psi_v(\boldsymbol{r},t)-\frac{1}{\mu_v}\nabla\times\frac{\partial}{\partial t}\boldsymbol{A}_v(\boldsymbol{r},t)\right]_{\tan}\\ =&\left[\frac{\partial}{\partial t}\boldsymbol{H}^{\mathrm{i}}(\boldsymbol{r},t)\right]_{\tan},\ \boldsymbol{r}\in S. \qquad (56)\end{aligned}$$

This form of PMCHW formulation has been solved by using MOT technique in [2]. Using (10) and (11), the time domain electric and magnetic current coefficients are expanded as

$$J_n(t) = \sum_{j=0}^{\infty} J_{n,j}\phi_j(st) \qquad (57)$$

$$M_n(t) = \sum_{j=0}^{\infty} M_{n,j}\phi_j(st) \qquad (58)$$

where $J_{n,j}$ and $M_{n,j}$ are the time domain current coefficients to be determined. Substituting (57) and (58) with (3)–(11) into (55) and (56), and following a similar procedure as that for (43), we have a matrix equation

$$\begin{bmatrix}\left[\alpha^E_{mn}\right] & \left[\beta^E_{mn}\right]\\ \left[\beta^H_{mn}\right] & \left[\alpha^H_{mn}\right]\end{bmatrix}\begin{bmatrix}[J_{n,i}]\\ [M_{n,i}]\end{bmatrix}=\begin{bmatrix}\left[\gamma^E_{m,i}\right]\\ \left[\gamma^H_{m,i}\right]\end{bmatrix},\quad i=0,1,2,\ldots,\infty \qquad (59)$$

where the impedance matrix elements in the left hand side are same to those used in (43) in the previous section and the elements related to the right hand side are obtained by replacing $J_{n,j}$ and $M_{n,j}$ instead of $e_{n,j}$ and $h_{n,j}$, respectively, and

$$V^E_m(t) = \int_S \boldsymbol{f}_m(\boldsymbol{r})\cdot\frac{\partial}{\partial t}\boldsymbol{E}^{\mathrm{i}}(\boldsymbol{r},t)dS \qquad (60)$$

$$V_m^H(t) = \int_S \boldsymbol{f}_m(\boldsymbol{r}) \cdot \frac{\partial}{\partial t} \boldsymbol{H}^{\mathrm{i}}(\boldsymbol{r}, t) dS. \tag{61}$$

By solving (59) with a marching-on in degree algorithm with M temporal basis functions, we can obtain the electric and magnetic current coefficients directly as given in (57) and (58) by replacing $M-1$ instead of ∞. The far field is obtained by the same expression as (52), where

$$\boldsymbol{A}_n = l_n \sum_q \boldsymbol{\rho}_n^q \frac{d}{dt} J_n(\tau_n^q) \tag{62}$$

$$\boldsymbol{F}_n = l_n \sum_q \boldsymbol{\rho}_n^q \frac{d}{dt} M_n(\tau_n^q). \tag{63}$$

The first derivative of the equivalent current coefficients is given in (25) with $M-1$ as the upper limit of summation over j instead of ∞.

4. NUMERICAL EXAMPLES

In this section, we present the numerical results for various representative 3-D dielectric scatterers with a ralative permittivity $\varepsilon_r = 2$, placed in the free space. In this section, c and η mean the speed of the wave propagation and the wave impedance of the free space, respectively. The scatterers are illuminated by a Gaussian plane wave, in which the electric and magnetic fields are given by

$$\boldsymbol{E}^{\mathrm{i}}(\boldsymbol{r}, t) = \boldsymbol{E}_0 \frac{4}{\sqrt{\pi} T} e^{-\gamma^2}, \qquad \boldsymbol{H}^{\mathrm{i}}(\boldsymbol{r}, t) = \frac{1}{\eta} \hat{\boldsymbol{k}} \times \boldsymbol{E}^{\mathrm{i}}(\boldsymbol{r}, t) \tag{64}$$

where $\gamma = (4/T)(ct - ct_0 - \boldsymbol{r} \cdot \hat{\boldsymbol{k}})$, $\hat{\boldsymbol{k}}$ is the unit vector in the direction of the wave propagation, T is the pulse width of the Gaussian impulse, and t_0 is a time delay which represents the time at which the pulse peaks at the origin. In this work, the field is incident from $\phi = 0°$ and $\theta = 0°$ with $\hat{\boldsymbol{k}} = -\hat{\boldsymbol{z}}$, and $\boldsymbol{E}_0 = \hat{\boldsymbol{x}}$. In the numerical computation, we use a Gaussian pulse of $T = 2\,\mathrm{lm}$ and $ct_0 = 4\,\mathrm{lm}$. The unit 'lm' denotes a light meter. One light meter is the length of time taken by the electromagnetic wave to travel 1 m in the free space. This pulse has a frequency spectrum of 500 MHz, which include several internal resonant frequencies of the structures to be analyzed. We set $s = 2 \times 10^9$ and $M = 80$, which is sufficient to get accurate solutions. All the solutions computed by our presented methods are compared with the inverse discrete Fourier transform (IDFT) of the solutions by the frequency-domain PMCHW formulation described in [10] in

the range of 0–500 MHz interval with 128 samples. All the far field solutions are θ- (or x-) component of electric fields taken along the backward direction ($+z$ axis) from the scatterers. In all legends of figures to be shown, 'FD-PMCHW' means IDFT solutions. 'PMCHW (I)' and 'PMCHW (II)' mean results computed by the formulation described in Section 2 and the alternative formulation in Section 3, respectively.

As a first example, we consider a dielectric sphere of radius 0.5 m centered at the origin. This has a total of 528 patches and 792 edges. Fig. 2 shows the transient response for the θ-directed electric and magnetic currents on the sphere at $\theta = 90°$ computed by the two presented methods and compares them with the IDFT solution. The current directions to be observed are designated by arrows on the common edges of triangle pairs. We can see that the solutions of two presented methods are stable and the agreement with the IDFT solutions is good. Fig. 3 presents the transient response for the back-scattered far field obtained by the two techniques just presented along with the Mie series solution and the IDFT solution. All the four solutions agree well as is evident from the figure.

Next, we show several examples of far field response from the various dielectric structures from Fig. 4 to Fig. 10. Fig. 4 presents the transient response for the far field from a dielectric hemisphere with the IDFT solution. The hemisphere has a radius of 0.5 m. This has a total of 432 patches and 648 edges. The transient responses for the far field computed by the proposed methods are stable. All the three solutions agree well as is evident from the figure. Fig. 5 shows the far field from a dielectric cone, which has a base of 0.5 m radius placed at $z = 0$ and 1 m height along the z-direction. This cone is divided into 624 triangular patches with a total number of 936 edges. Back-scattered far-zone field obtained using the two proposed method are stable. A good agreement in the three results is evident for this example. Next the structure of the dielectric double cones is considered, which is shown in Fig. 6. The height of the cones along z-direction is 1 m and the radius at $z = 0$ is 0.5 m. This structure is divided into 528 triangular patches with a total number of 792 edges. In this figure, the back-scattered fields computed by our proposed methods are compared with the IDFT result.

The next example is the structure of a hemisphere terminated by a cone, which is shown in Fig. 7. The radius of the hemisphere is 0.5 m and the height of the cone along the z-direction is 0.5 m. This structure is divided into 528 triangular patches with a total number of 792 edges. In Fig. 7, the back-scattered fields are computed by our proposed methods and are compared with the IDFT results. The next structure to be analyzed is the dielectric cylinder centered at the origin,

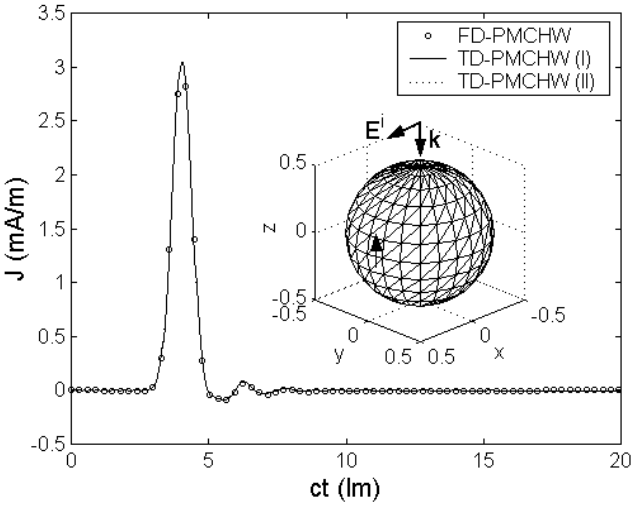

(a)

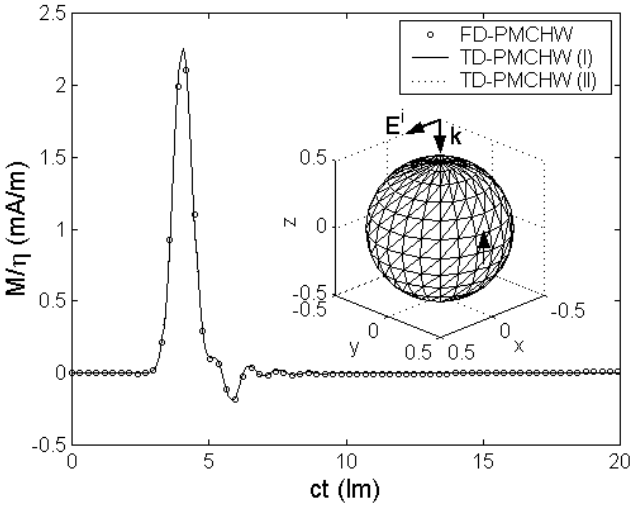

(b)

Figure 2. Transient current responses on the dielectric sphere at $\theta = 90°$. (a) Electric current density at $\phi = 7.5°$. (b) Magnetic current density at $\phi = 172.5°$.

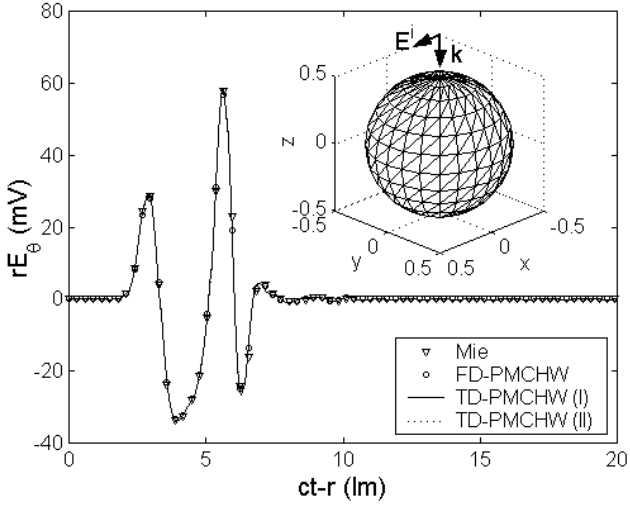

Figure 3. Backward scattered field from the dielectric sphere along the $+z$ direction. Number of edges $N = 792$.

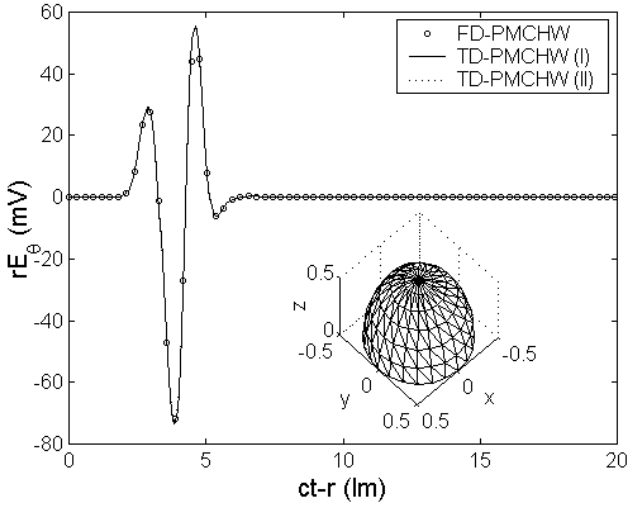

Figure 4. Backward scattered field from the dielectric hemisphere along the $+z$ direction. Number of edges $N = 648$.

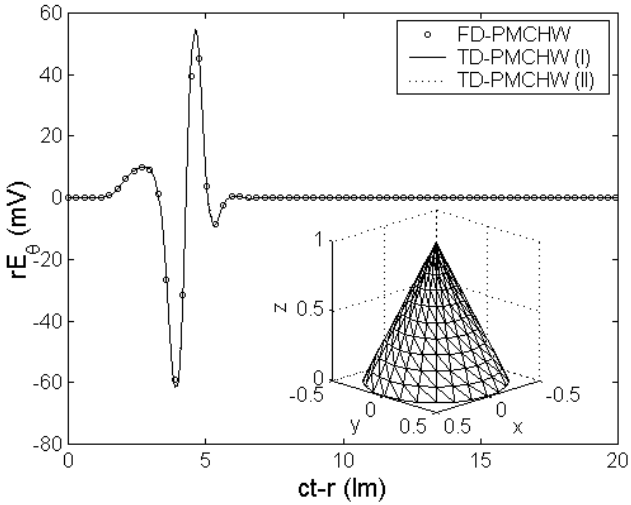

Figure 5. Backward scattered field from the dielectric cone along the $+z$ direction. Number of edges $N = 936$.

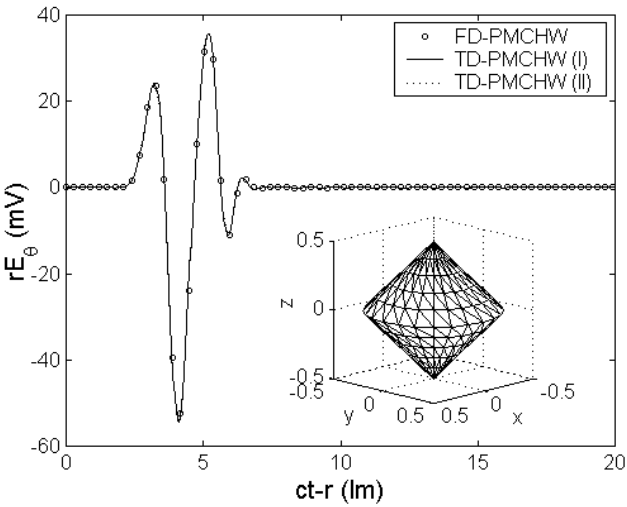

Figure 6. Backward scattered field from the dielectric double cones along the $+z$ direction. Number of edges $N = 792$.

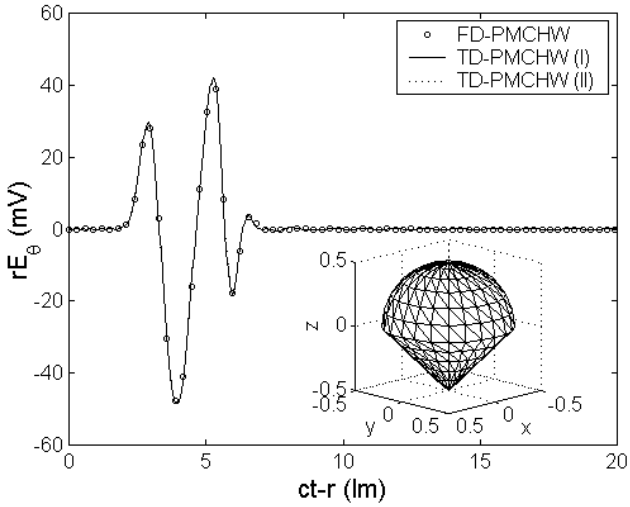

Figure 7. Backward scattered field from the dielectric hemisphere-cone along the $+z$ direction. Number of edges $N = 792$.

which is shown in Fig. 8. The radius of the cylinder is 0.5 m and the height along the z-direction is 1 m. This structure is divided into 720 triangular patches with a total number of 1,080 edges. In Fig. 8, the back-scattered fields computed by our proposed methods are compared with the IDFT results.

The next example is the structure of a hemisphere terminated by a cylinder, which is shown in Fig. 9. The radius of the hemisphere is 0.5 m and the height of the cylinder along z-direction is 0.5 m. This structure is divided into 624 triangular patches with a total number of 936 edges. In Fig. 9, the back-scattered fields computed by our proposed methods are compared with the IDFT results. As a final example, the dielectric body of a cone-cylinder is considered. The radius of the cylinder is 0.5 m and the height of the cylinder along the z-direction is 0.5 m. The heigh of the cone along z-direction is 0.5 m. This structure is divided into 576 triangular patches with a total number of 864 edges. Fig. 10 shows the back-scattered fields computed by our proposed methods and compares with the IDFT result. The agreement of all the solutions computed by the proposed methods and the IDFT solutions is excellent and it is difficult to distinguish between the two presented results.

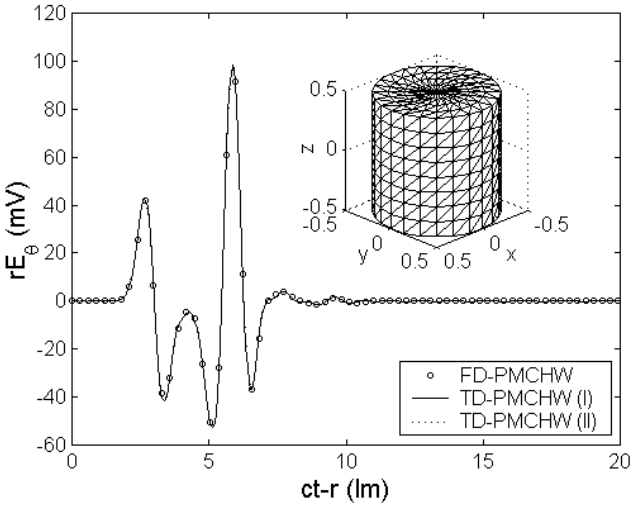

Figure 8. Backward scattered field from the dielectric cylinder along the $+z$ direction. Number of edges $N = 1,080$.

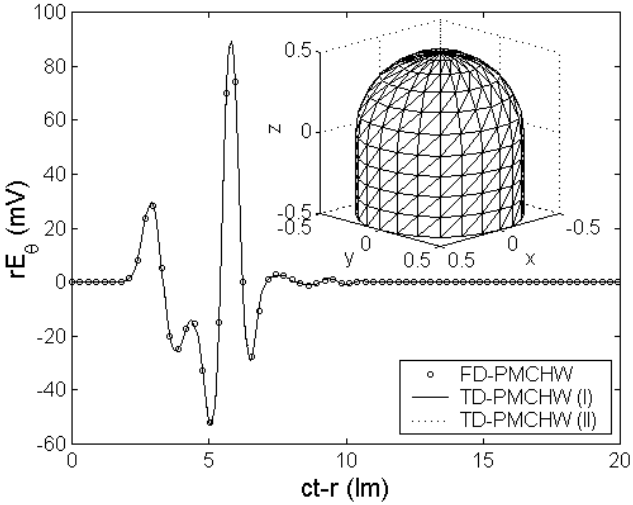

Figure 9. Backward scattered field from the dielectric hemisphere-cylinder along the $+z$ direction. Number of edges $N = 936$.

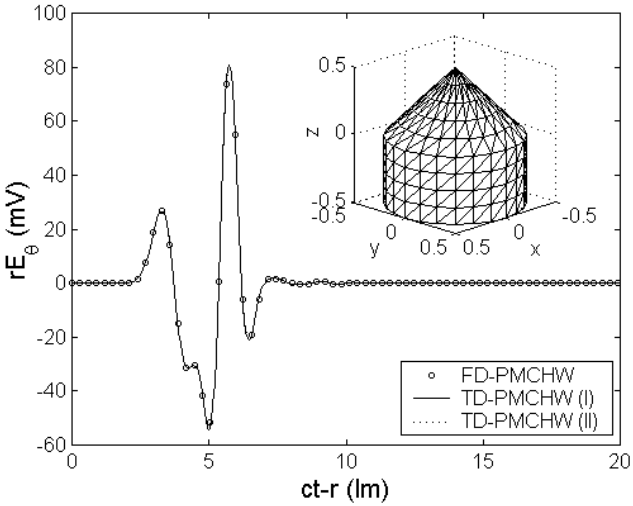

Figure 10. Backward scattered field from the dielectric cone-cylinder along the $+z$ direction. Number of edges $N = 864$.

5. CONCLUSION

We have presented a novel method to solve the time-domain PMCHW integral equations for scattering from three-dimensional arbitrarily shaped dielectric structures. To apply a MoM procedure, we used triangular patch functions as spatial basis and testing functions. We introduced a temporal basis function set derived from the Laguerre polynomials and exponential functions. With the representation of the derivative of the transient coefficient in an analytic form, the temporal derivative in the integral equation can be treated analytically. The advantage of the proposed method is to guarantee late-time stability. Transient equivalent currents and far field obtained by the two methods presented in this paper are accurate and stable. The agreement between the solutions obtained using the two proposed methods and the IDFT of the frequency-domain solution is excellent.

REFERENCES

1. Rao, S. M., *Time Domain Electromagnetics*, Academic Press, 1999.
2. Vechinski, D. A., S. M. Rao, and T. K. Sarkar, "Transient scattering from three-dimensional arbitrary shaped dielectric

bodies," *J. Opt. Soc. Amer.*, Vol. 11, No. 4, 1458–1470, April 1994.

3. Rao, S. M. and T. K. Sarkar, "Implicit solution of time-domain integral equations for arbitrarily shaped dielectric bodies," *Microwave Opt. Technol. Lett.*, Vol. 21, No. 3, 201–205, May 1999.
4. Sarkar, T. K., W. Lee, and S. M. Rao, "Analysis of transient scattering from composite arbitrarily shaped complex structures," *IEEE Trans. Antennas Propagat.*, Vol. 48, No. 10, 1625–1634, Oct. 2000.
5. Chung, Y.-S., T. K. Sarkar, and B. H. Jung, "Solution of a time-domain magnetic-field integral equation for arbitrarily closed conducting bodies using an unconditionally stable methodology," *Microwave Opt. Technol. Lett.*, Vol. 35, No. 6, 493–499, Dec. 2002.
6. Rao, S. M., D. R. Wilton, and A. W. Glisson, "Electromagnetic scattering by surfaces of arbitrary shape," *IEEE Trans. Antennas Propagat.*, Vol. 30, No. 3, 409–418, May 1982.
7. Wilton, D. R., S. M. Rao, A. W. Glisson, D. H. Schaubert, O. M. Al-Bundak, and C. M. Butler, "Potential integrals for uniform and linear source distributions on polygonal and polyhedral domains," *IEEE Trans. Antennas Propagat.*, Vol. 32, No. 3, 276–281, March 1984.
8. Poularikas, A. D., *The Transforms and Applications Handbook*, IEEE Press, 1996.
9. Gradshteyn, I. S. and I. M. Ryzhik, *Table of Integrals, Series, and Products*, Academic Press, New York, 1980.
10. Jung, B. H., T. K. Sarkar, and Y.-S. Chung, "A survey of various frequency domain integral equations for the analysis of scattering from three-dimensional dielectric objects," *J. of Electromagn. Waves and Applicat.*, Vol. 16. No. 10, 1419–1421, 2002.

Baek Ho Jung was born in Korea in 1961. He received the B.S., M.S., and Ph.D. degrees in Electronic and Electrical Engineering from Kyungpook National University, Taegu, Korea, in 1986, 1989, and 1997, respectively. From 1989 to 1994, he was a researcher at Agency for Defense Development in Korea. Since 1997, he has been a Lecturer and currently an Assistant Professor in the Department of Information and Communication Engineering, Hoseo University, Asan, Korea. He is now in Syracuse University, NY as a visiting scholar from 2001 to 2003. His current interests are in computational electromagnetics and wave propagation.

Tapan Kumar Sarkar received the B.Tech. degree from the Indian Institute of Technology, Khatagpur, India, in 1969, the M.Sc.E. degree from the University of New Brunswick, Fredericton, Canada, in 1971, and the M.S. and Ph.D. degrees fiom Syracuse University; Syracuse, New York in 1975. From 1975 to 1976 he was with the TACO Division of the General Instruments Corporation. He was with the Rochester Institute of Technology, Rochester, NY, ftom 1976 to 1985. He was a Reseatch Fellow at the Gordon McKay Laboratory, Harvatd Univasity, Cambridge, MA, from 1977 to 1978. He is now a Professor in the Depattment of Electrical and Computer Engineering, Syracuse University; Sytacuse, NY. His current reseatch interests deal with numerical solutions of operator equations arising in electromagnetics and signal processing with application to system design. He has authored or coauthored more than 210 journal articles and numerous conference papers and has written chapters 28 books and ten books including the latest one "Iterative and Self Adaptive Finite-Elements in Electromagnetic Modeling" which was published in 1998 by Artech House. He was an Associate Editor for feature articles of the EEE Antennas and Propagation Society Newsletter, and he was the Technical Program Chairman for the 1988 IEEE Antennas and Propagation Society International Symposium and URSI Radio Science Meeting. He is on the editorial board of Journal of Electromagnetic Waves and Applications and Microwave and Optical Technology Letters. He received the title Docteur Honoris Causa from Universite Blaise Pascal, Clermont Ferrand, France in 1998 and the medal of the City Clermont Ferrand, France in 2000.

Young-seek Chung received the B.S., M.S., and Ph.D. degrees in electrical engineering from the Seoul National University, Seoul, Korea, in 1989, 1991, and 2000, respectively. From 1991 to 1996, he was with the Living System Laboratory, LG Electronics. From 1998 to 2000, he was a Teaching Assistant of electrical engineering with the Seoul National University. From 2001 to 2002, he was with Syracuse University, Syracuse, NY as a post-doctor. Since 2003, he has been a faculty member with the Department of Communication Engineering, Myongji University, Kyunggi, Korea. His current interests are numerical analysis and inverse scattering using time-domain methods.